assistance with the spectrofluorometer, N. Zachara for assistance with the SMART analysis, and A. Guerrerio for valuable assistance with the design of the anisotropy experiments and data analysis. This work was supported by grants from the National Institutes of Health.

Correspondence should be addressed to J.M.B. *email: jberg@jhmi.edu*

Received 7 August, 2000; accepted 3 October, 2000.

1. van den Bosch, H., Schutgens, R.B.H., Wanders, R.J.A. & Tager, J.M. *Annu. Rev. Biochem.* **61**, 157–197 (1992).
2. Gould, S.J. & Valle, D. *Trends Genet.* **16**, 340–345 (2000).
3. Gould, S.J., Keller, G.A., Hosken, N., Wilkinson, J. & Subramani, S. *J. Cell Biol.* **108**, 1657–1664 (1989).
4. Dodt, G. *et al. Nature Genet.* **9**, 115–125 (1995).
5. Terlecky, S.R., Nuttley, W.M., McCollum, D., Sock, E. & Subramani, S. *EMBO J.* **14**, 3627–3634 (1995).
6. Gatto, G.J., Jr., Geisbrecht, B.V., Gould, S.J. & Berg, J.M. *Proteins* **38**, 241–246 (2000).
7. Goebl, M. & Yanagida, M. *Trends Biochem. Sci.* **16**, 173–177 (1991).
8. Blatch, G.L. & Lässle, M. *BioEssays* **21**, 932–939 (1999).
9. Lamb, J.R., Tugendreich, S. & Hieter, P. *Trends Biochem. Sci.* **20**, 257–259 (1995).
10. Hirano, T., Kinoshita, N., Morikawa, K. & Yanagida, M. *Cell* **60**, 319–328 (1990).
11. Sikorski, R.S., Boguski, M.S., Goebl, M. & Hieter, P. *Cell* **60**, 307–317 (1990).
12. Das, A.K., Cohen, P.W. & Barford, D. *EMBO J.* **17**, 1192–1199 (1998).
13. Scheufler, C. *et al. Cell* **101**, 199–210 (2000).
14. Schliebs, W. *et al. J. Biol. Chem.* **274**, 5666–5673 (1999).
15. Swinkels, B.W., Gould, S.J. & Subramani, S. *FEBS Lett.* **305**, 133–136 (1992).
16. Braverman, N., Dodt, G., Gould, S.J. & Valle, D. *Hum. Mol. Genet.* **7**, 1195–1205 (1998).
17. Shimozawa, N. *et al. Biochem. Biophys. Res. Commun.* **262**, 504–508 (1999).
18. Blobel, G. & Dobberstein, B. *J. Cell Biol.* **67**, 835–851 (1975).
19. Keenan, R.J., Freymann, D.M., Walter, P. & Stroud, R.M. *Cell* **94**, 181–191 (1998).
20. Clemons, W.M., Jr., Gowda, K., Black, S.D., Zwieb, C. & Ramakrishnan, V. *J. Mol. Biol.* **292**, 697–705 (1999).
21. Batey, R.T., Rambo, R.P., Lucast, L., Rha, B. & Doudna, J.A. *Science* **287**, 1232–1239 (2000).
22. Conti, E., Uy, M., Leighton, L., Blobel, G. & Kuriyan, J. *Cell* **94**, 193–204 (1998).
23. Opperdoes, F.R. *Annu. Rev. Microbiol.* **41**, 127–151 (1987).
24. Keller, G.A. *et al. J. Cell Biol.* **114**, 893–904 (1991).
25. de Walque, S., Kiel, J.A., Veenhuis, M., Opperdoes, F.R. & Michels, P.A. *Mol. Biochem. Parasitol.* **104**, 106–119 (1999).
26. Geisbrecht, B.V., Zhang, D., Schulz, H. & Gould, S.J. *J. Biol. Chem.* **274**, 21797–21803 (1999).
27. Otwinowski, Z. & Minor, W. *Methods Enzymol.* **276**, 307–326 (1997).
28. Terwilliger, T.C. & Berendzen, J. *Acta Crystallogr. D* **55**, 849–861 (1999).
29. Collaborative Computational Project, Number 4. *Acta Crystallogr. D* **50**, 760–763 (1994).
30. Cowtan, K. Joint CCP4 and ESF–EACBM Newsletter. *Protein Crystallogr.* **31**, 34–38 (1994).
31. Jones, T.A., Zou, J.Y., Cowan, S.W. & Kjeeldgard, M. *Acta Crystallogr. A* **47**, 110–119 (1991).
32. Brünger, A.T. *et al. Acta Crystallogr. D* **54**, 905–921 (1998).
33. Kraulis, P.J. *J. Appl. Crystallogr.* **24**, 946–950 (1991).
34. Esnouf, R.M. *J. Mol. Graphics* **15**, 132–134 (1997).
35. Nicholls, A., Sharp, K.A. & Honig, B. *Proteins* **11**, 281–296 (1991).

A *de novo* designed helix-turn-helix peptide forms nontoxic amyloid fibrils

Youcef Fezoui[1], Dean M. Hartley[1], Dominic M. Walsh[1], Dennis J. Selkoe[1], John J. Osterhout[2] and David B. Teplow[1]

[1]Department of Neurology (Neuroscience), Harvard Medical School, and Center for Neurologic Diseases, Brigham and Women's Hospital, Boston, Massachusetts 02115, USA. [2]Rowland Institute for Science, Cambridge, Massachusetts 02142,USA

We report here that a monomeric *de novo* designed α-helix-turn-α-helix peptide, αtα, when incubated at 37 °C in an aqueous buffer at neutral pH, forms nonbranching, protease resistant fibrils that are 6–10 nm in diameter. These fibrils are rich in β-sheet and bind the amyloidophilic dye Congo red. αtα fibrils thus display the morphologic, structural, and tinctorial properties of authentic amyloid fibrils. Surprisingly, unlike fibrils formed by peptides such as the amyloid β-protein or the islet amyloid polypeptide, αtα fibrils were not toxic to cultured rat primary cortical neurons or PC12 cells. These results suggest that the potential to form fibrils under physiologic conditions is not limited to those proteins associated with amyloidoses and that fibril formation alone is not predictive of cytotoxic activity.

The amyloidoses comprise a group of disorders characterized by aberrant protein folding and assembly that results in the accumulation of insoluble protein fibrils. Amyloid deposition leads to cell and organ dysfunction, and in many cases, to death. At least 17 different proteins and polypeptides form amyloid deposits *in vivo*[1]. Even though these proteins are nonhomologous and have diverse tertiary and quaternary structures, all can polymerize *in vitro* into fibrils with similar ultrastructural appearance and tinctorial properties. In addition, soluble oligomeric and polymeric assemblies of amyloid proteins may be toxic, as is the case for the amyloid β-protein (Aβ)[2–5]. Certain 'nonamyloidogenic' proteins can form fibrils when partially denatured by incubation at subphysiologic pH or in the presence of organic solvents, suggesting that fibril formation might be an intrinsic property of most proteins[6–8]. We report here that αtα, a *de novo* designed 38-residue α-helical peptide with a protein-like sequence and a stable tertiary fold, forms amyloid-type fibrils when incubated at 37 °C in an aqueous buffer at neutral pH. Surprisingly, these fibrils were nontoxic to cultured neuronal cells. αtα may be a useful peptide model for the detailed biophysical study of α-helix to β-strand transitions occurring under aqueous conditions and for determining the structural factors within fibril assemblies that mediate cytotoxic activity.

Fibril formation by αtα

During studies of the fibrillogenesis of Aβ, we sought a stable, nonamyloidogenic peptide to use as a 'negative' control. Prior work suggested that αtα, a *de novo* designed monomeric 38-residue α-helix-turn-α-helix peptide with a protein-like sequence and a stable tertiary structure, would be ideal. αtα was developed as a model for the study of protein folding intermediates and was designed to consist of two helices connected by a turn region[9]. The NMR derived solution structure of αtα shows precisely this conformation[10]. αtα is monomeric immediately after dissolution in buffers of pH 3.6, 7.4, and 10.5 (ref. 9). At pH 3.6 and 10.5, at concentrations up to 400 μM, αtα showed no aggregation after eight weeks of incubation at 37 °C (data not shown). Surprisingly, at neutral pH, a 60 μM solution of αtα produced fibrils after two days of incubation at 37 °C. Negative staining and electron microscopy (EM) revealed nonbranching fibril assemblies 6–10 nm in width, which varied in length from 200–1200 nm (Fig. 1*a*). These assemblies were composed of two or more filaments, each 3–3.5 nm in diameter, and their structures had the appearance of narrow ribbons, some of which displayed helical twists of irregular pitch. These types of structures also form during the assembly of Aβ and islet amyloid polypeptide (IAPP)[11]. However, the rope-like, bifilar structures commonly

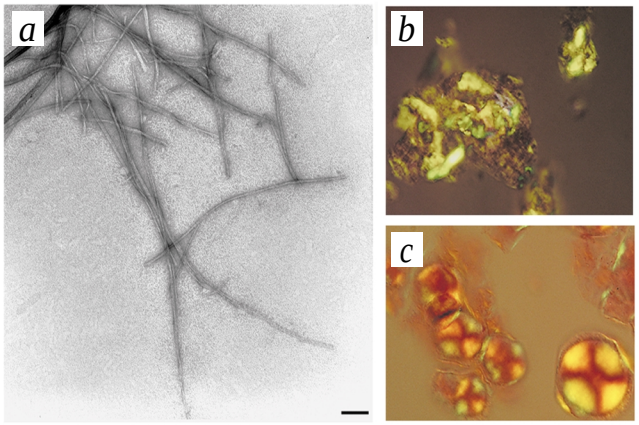

Fig. 1 Fibril formation by αtα. ***a***, Negative staining and electron microscopy of αtα fibrils (scale bar = 100 nm). ***b***, Congo red staining of αtα fibrils (magnification = 160×). ***c***, Congo red staining of large fibril aggregates (magnification = 80×). The data shown are representative of those obtained in each of three independent experiments.

seen in fibrils of Aβ and IAPP were not observed for αtα. As shown for other nucleation-dependent polymerization processes[12], addition of 5% (w/w) preformed αtα fibrils to freshly dissolved, monomeric αtα solutions at pH 7.4 accelerated fibril formation (data not shown). However, no new fibril formation was observed when experiments were done at pH 3.6 or 10.5.

Tinctorial properties of αtα fibrils

To determine whether the αtα fibrils had tinctorial properties characteristic of amyloid, Congo red binding studies were performed periodically during a two day incubation of αtα in 5 mM sodium phosphate, 100 mM NaC1 (PBS) at pH 7.4. As fibril formation proceeded, the wavelength of the absorption maximum shifted from ~487 nm to ~505 nm and the absolute absorbance approximately doubled (data not shown). Congo red treated, aggregated fibrils produced a bright, yellow-green color when examined using crosspolarized light (Fig. 1*b*). This staining pattern is found *in vivo* in deposits formed in a wide variety of amyloidoses[13]. When the fibril aggregates were sufficiently large, a characteristic segmented, yellow-green pattern of birefringence was also observed (Fig. 1*c*). Taken together, these data demonstrate that αtα forms amyloid fibrils in aqueous solution at neutral pH.

Protease sensitivity of αtα fibrils

One of the properties of amyloid fibrils, which may inhibit their catabolism, is protease resistance. We used proteinase K (PK) to determine the protease resistance of nonfibrillar and fibrillar αtα. Monomeric αtα was extremely sensitive to PK. Within 2 min, 85% had been digested, and by 5 min, the level of digestion was >95% (data not shown). In contrast, αtα fibrils showed marked PK resistance, with ~75% remaining intact after 45 min of digestion (data not shown). The incorporation of αtα monomers into fibrils is thus associated with a significant increase in the resistance of the molecule to proteolysis, as is typical of the monomers composing other amyloids.

Conformational studies of αtα

To correlate the conformational properties of αtα with its ability to form fibrils, circular dichroism (CD) spectroscopy was used to determine the secondary structure of αtα at 37 °C and pH 3.6, 7.4, and 10.5 (Fig. 2*a*). In addition, the α-helix stability of αtα at these three pHs was examined by measuring the molar ellipticity at 222 nm as a function of temperature (Fig. 2*b*). The data showed that increasing the pH from 3.6 to 10.5 induced a conformational transition from a highly helical and thermally stable structure (pH 3.6, 80% helix) to a largely disordered structure (pH 10.5, 78% random coil (RC)). At pH 7.4, a structure formed that contained 50% helix (Fig. 2*a*) and displayed a temperature denaturation midpoint 10 °C lower than that at pH 3.6 (Fig. 2*b*, arrows). The isodichroic point at 204 nm (Fig. 2*a*) suggests a two-state transition. However, neither the unfolded (pH 10.5) nor the folded (pH 3.6) forms of αtα produce fibrils; therefore, at least one other state exists at neutral pH, one that is prone to fibril formation.

An explanation for the decrease in helicity and stability at neutral pH could be a decrease in the intrinsic helix propensity (s value) of Glu in its deprotonated state[14,15] and the fact that Glu packs less favorably with hydrophobic residues in the helix–helix interface of αtα when it is deprotonated. An

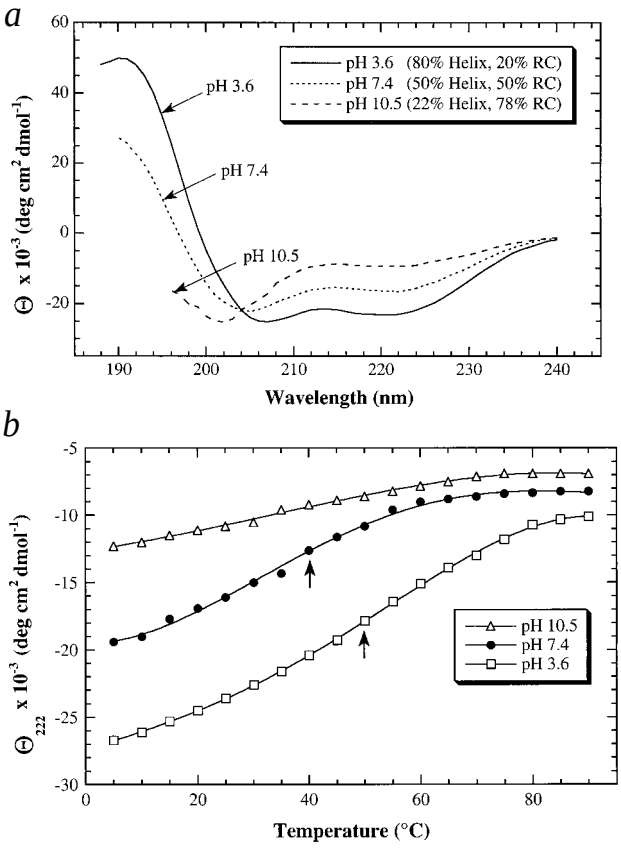

Fig. 2 Conformational stability of αtα. ***a***, pH dependent unfolding of αtα as measured by CD spectroscopy. ***b***, Thermal unfolding of αtα. Temperature unfolding curves were obtained by monitoring mean residue ellipticity at 222 nm. At pH 7.4, αtα displayed its lowest content of α-helix at a temperature ~20 °C lower than that displayed at pH 3.6 (60 °C *versus* 80 °C). In addition, the midpoint of denaturation was 10 °C lower at pH 7.4 than at pH 3.6 (40 °C *versus* 50 °C, see arrows). At pH 10.5, αtα was largely disordered, even at the lowest temperature (5 °C).

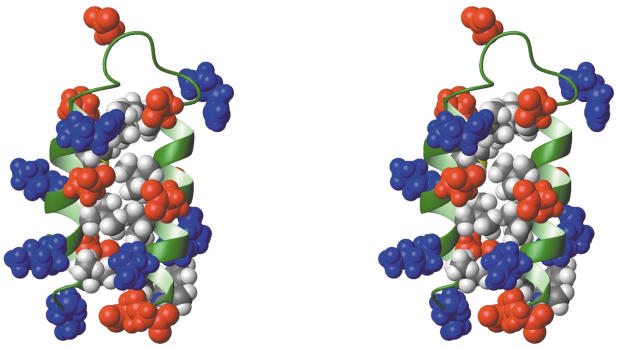

Fig. 3 Stereo view of αtα showing the charged residues located near the hydrophobic interface. The helices of αtα are rendered as green ribbons and the side chains of the charged and hydrophobic residues are rendered as space filling models. The seven positively charged amino acids (three Arg and four Lys) are shown in blue. The six negatively charged Glu residues are shown in red. The N-terminal succinyl-Asp (lower right) and the Asp located in the turn (top) are also colored red. The hydrophobic side chains are shown in gray and white. The figure represents the NMR derived conformation closest to the average structure[10]. The drawing was produced with MOLMOL[31].

important aspect of the design of αtα was the positioning of charged residues (Fig. 3). The six Glu residues were positioned near the helix–helix interface so that the aliphatic portions of their side chains could pack against neighboring hydrophobic residues[16]. Decreases in the s value and the hydrophobic interactions of Glu would destabilize the helices and could expose hydrophobic side chains to the solvent. These partially unfolded, less stable conformers would likely have an increased propensity to aggregate. A decrease in helical stability at neutral pH due to Glu has, in fact, also been reported in studies of dimeric helical peptides such as the GCN4 leucine zipper coiled coil[17] and a *de novo* designed coiled coil peptide[18].

Our results support the conclusion that partially folded conformers of αtα, populated at pH 7.4, mediate fibril formation, whereas the stable, folded forms of αtα present at pH 3.6, or the disordered conformers formed at pH 10.5, do not support fibril formation. These findings are consistent with the results of studies of the effects of trifluoroethanol (TFE) on fibril formation by acylphosphatase, which show that relatively low concentrations of TFE can accelerate fibril formation, but that at higher concentrations, helical conformations are stabilized and unable to convert into β-sheets[6]. In fact, for αtα, we have found that fibril formation is suppressed by addition of TFE during incubation of a 60 μM solution at neutral pH and 37 °C. At or above 30% (v/v) TFE, αtα exhibits an elevated and constant helical content of ~75%, is Congo red negative, and produces transparent solutions with no evidence of aggregation, even after two weeks of incubation. From 0–30% TFE, fibril formation is retarded in a concentration-dependent manner, but β-sheet formation, Congo red binding, and solution turbidity all occur by no later than 10 days.

Conformation of αtα during assembly

In an effort to understand the relationship between the secondary structure and the assembly state of αtα, temporal changes in CD spectra were correlated with oligomerization state and electron microscopically determined morphology.

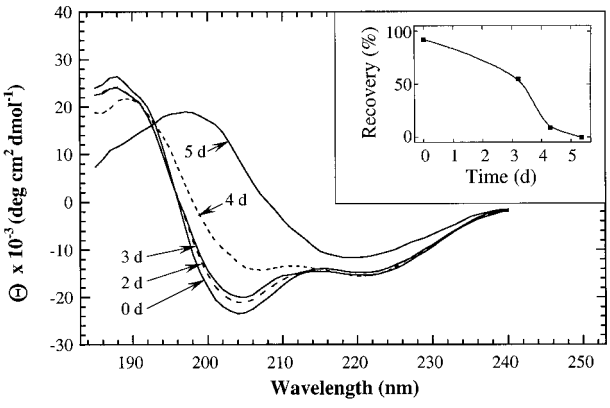

The CD spectra of αtα at pH 7.4 following 0, 2, 3, 4 and 5 days of incubation at 37 °C are presented in Fig. 4. Deconvolution of the CD spectrum obtained immediately after peptide dissolution showed 49% α-helix and 51% RC. Small changes in secondary structure were observed during the first three days. One day later, β-structure (12%) was apparent and a decrease in RC content was observed. After five days, the spectrum of αtα showed one minimum at 218 nm, a feature consistent with a calculated level of β-structure of 72%.

At each time point, the amounts of αtα oligomers were determined by filtration through 10 kDa membranes, followed by amino acid analysis (Fig. 4, inset). Based on a nominal molecular mass of 4,440 for αtα, molecules passing through the 10 kDa membrane should be monomeric or dimeric. Immediately after dissolution, 92% of αtα passed through the membrane. After three days, 55% of αtα was found in the filtrate. Because the corresponding CD spectrum on day 3 revealed only α-helix and RC structures, these data argue that αtα oligomerization occurs prior to detectable β-strand formation. In fact, electron microscopic examination of the samples revealed no fibrillar assemblies during the first three days of incubation (data not shown). Some short fibrils were detected after four days, a time point at which β-structure became apparent by CD and only ~9% of αtα passed through the filter. By day 5, numerous long fibrils were observed, consistent with the high content of β-sheet observed by CD, and essentially no αtα peptide passed through the filter.

Modeling αtα fibrillogenesis

Our results are consistent with a model of αtα fibrillogenesis in which the initial step of the process involves destabilization of helix–helix interactions within the folded αtα monomer. The resulting intermediate is a partially unfolded conformer that may unfold completely to yield an unstructured species or may undergo intermolecular association to form oligomeric αtα assemblies. No significant change in the helical content of the αtα population occurs during this latter process. A β-sheet transition within the largely helical oligomeric αtα population then leads to the formation of oligomers containing extended β-sheets and of classical amyloid-like fibrils with cross-β secondary structure. It is possible that the mechanism of the helix

Fig. 4 Temporal changes in the secondary structure of αtα during fibrillogenesis. The data shown are representative of those obtained in each of three independent experiments. Inset: quantification of trimeric and higher order oligomers. At each time point, aliquots of the αtα sample were removed and filtered through 10 kDa MWCO filters. The percent recovery of αtα in the filtrate was determined by amino acid analysis on aliquots from the starting material and from the filtrate.

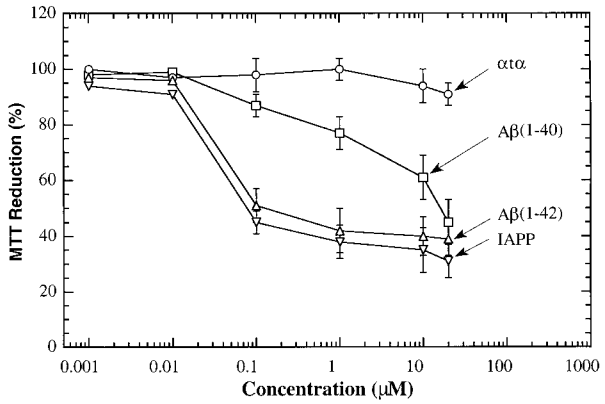

Fig. 5 Effect of amyloid peptides on MTT formazan formation by PC12 cells. PC12 cells were incubated overnight with fibrillar αtα, Aβ(1–40), Aβ(1–42), IAPP, or medium alone (negative control). MTT was then added for 3 h, after which the cells were solubilized. Aβ(1–40), Aβ(1–42), and IAPP were used as positive controls. Data are expressed as average MTT reduction ± S.D. (n = 6) relative to cells treated with medium alone (which was made to equal 100%). The graph presents results from one experiment, but is representative of results from at least three independent experiments.

to strand transition is the formation of a critical long range interaction (equivalent to a nucleus) in the oligomer that would favor formation and stabilization of β-sheet structure.

Our model of αtα fibril assembly may have relevance for understanding the structural reorganization and assembly of helix-containing proteins and peptides[19,20]. The model may also be relevant to amyloid formation by transthyretin and lysozyme, in which the formation of a partially unfolded intermediate precedes fibril assembly[1,21,22]. We note that the Mihara group has used a 34-residue peptide conjugate (2α) to study α-helix to β-strand transitions[23,24]. This peptide differs significantly from αtα in that it is constructed from two parallel diheptad sequences that are linked by a C-terminal disulfide bond and whose N-termini are acylated with hydrophobic groups. These 'hydrophobic defects' are postulated to induce the α to β transition[25], rather than the intrinsic action of native amino acids within the peptide, as is observed in αtα fibrillogenesis.

Biological activity of αtα fibrils

One of the most clinically important properties of amyloidogenic proteins is cytotoxicity. For example, studies have shown that Aβ fibrils are neurotoxic *in vitro* and that Aβ fibrils injected into nonhuman primates induce Alzheimer's disease-associated changes[26]. To determine whether αtα fibrils were neurotoxic, lactate dehydrogenase (LDH) release assays, which measure cell death, were performed following incubation of peptide with cultured rat primary cortical neurons. αtα was preincubated for 0, 1, 3 or 6 days to provide prefibrillar and fibrillar samples. Aβ(1–40), used as a positive control, was preincubated for 0 or 3 days. Relative to cells treated with medium, no significant LDH release was observed from cells treated with prefibrillar or fibrillar αtα (data not shown). In contrast, cells treated with Aβ fibrils showed significant cell death ($p < 0.0001$). Substantial LDH release requires loss of plasma membrane integrity, thus any physiologic insult that does not cause membrane rupture would appear benign by this assay. To examine whether αtα fibrils might affect the normal physiology of cells without altering membrane integrity, we studied the effects of αtα treatment on reduction of the redox active dye 3-(4,5-dimethylthiazol-2-yl)-2,5-diphenyltetrazolium bromide (MTT) by PC12 cells. Here, MTT reduction was used a general indicator of physiologic stress[27]. As positive controls, Aβ(1–40), Aβ(1–42), and IAPP were also assayed. IAPP is a 37-amino acid peptide that forms pancreatic amyloid deposits in patients with type 2 diabetes[28]. We found that Aβ(1–40), Aβ(1–42), and IAPP all produced significant, concentration-dependent decreases in the levels of reduced MTT, whereas αtα fibrils had little effect (Fig. 5).

The lack of toxicity of αtα fibrils in experiments using primary neurons and PC12 cells was surprising in light of the clear toxic effects of the Aβ and IAPP fibrils. One explanation is rapid fibril dissociation during coincubation with the cells. However, centrifugation of the culture medium after one day of incubation produced a pellet in which αtα fibrils were readily found upon examination by electron microscopy (data not shown). Given that fibrils were present at least during the initial phases of the LDH assay, and throughout the entire MTT assay, it is probable that the intrinsic toxic potential of αtα fibrils differs from those of Aβ and IAPP fibrils. At a gross morphologic level, αtα fibrils do not display the bifilar rope-like structures often seen in Aβ and IAPP fibrils, but rather tend to form ribbon-like lateral arrays of narrow filaments. These narrow filaments and their arrays appear to lack the toxic potential of the thicker, bundled filaments formed by Aβ and IAPP. It is possible that αtα fibrils do not interact effectively with cell surface targets mediating cytotoxicity.

Conclusions

αtα is a *de novo* designed peptide with a protein-like sequence and a stable helical conformation that forms amyloid-type fibrils. αtα fibril assembly provides a simple but powerful model system for elucidating key mechanistic features of the conformational transitions and intermolecular associations occurring during the folding and polymerization of helix-containing proteins and peptides. We have shown here that β-sheet structure is not required for the association process to start and that partially folded intermediates, containing no observable β-sheet structure, can mediate the initial stages of fibril formation. Importantly, as exemplified by αtα, fibril formation alone is not predictive of cytotoxic activity. Fibrillogenesis *per se* thus does not produce generic assemblies with common biological properties. Rather, each type of fibril may have unique physical and biological characteristics related to its quaternary structure, the spatial organization and chemical reactivity of its exposed amino acid side chains, and its thermodynamic stability. Comparative studies of the interactions of nontoxic (αtα) and toxic (Aβ, IAPP, etc.) fibrils with cells offer the possibility of elucidating the molecular bases for fibril toxicity. Studies such as these will facilitate the rational design of therapeutic agents for use in treating amyloidoses.

Methods

Peptides. αtα (succinyl-DWLKARVEQELQALEARGTDSNAELRAMEAKLKAEIQK-NH_2), Aβ(1–40), and Aβ(1–42) were synthesized using 9-fluorenylmethoxycarbonyl (FMOC) chemistry and purified by reverse phase HPLC, essentially as described[9,29]. IAPP (NH_2-KCNTATCATQRLANFLVHSSNNFGAILSSTNVGSNTY-NH_2) was obtained from Calbiochem-Novabiochem (San Diego, California).

Electron microscopy. EM was performed as described[29]. Briefly, 60 μM αtα in 5 mM sodium phosphate, pH 7.4, 100 mM NaCl (PBS), was incubated for two days at 37 °C and then aliquots were applied to carbon coated Formvar grids, fixed with glutaralde-

hyde, and stained with uranyl acetate. Samples were examined using a JEOL 1200 EX transmission electron microscope.

Congo red binding and birefringence. Congo red binding was assayed essentially as described[30]. For Congo red birefringence experiments, 60 and 200 μM αtα solutions in PBS, pH 7.4, were incubated at 37 °C for two and one day, respectively. Following incubation, the samples were centrifuged at 16,000 *g* for 30 min and the pellets were stained with Congo red for 5 min at ambient temperature. The samples then were centrifuged at 16,000 *g* for 2 min, the supernates removed, the pellets washed twice with 100 μl of 50% ethanol, resuspended in 50 μl of PBS, and then spread evenly onto glass slides. The slides were examined with a light microscope using crossed polarizers.

Proteolysis. Fibrillar αtα was produced by incubation of 100 μM peptide in PBS, pH 7.4, for two days at 37 °C. Following incubation, the fibrils were pelleted at 16,000 *g* for 30 min, then resuspended in one volume of 50 mM Tris-HCl, pH 7.4, and sonicated for 5 min. PK was then added to the sonicated peptide to yield an enzyme:substrate ratio of 1:10 (w/w) and digestion was allowed to proceed at 37 °C. Monomeric αtα was digested under identical conditions, immediately following dissolution in 50 mM Tris-HCl, pH 7.4. Aliquots were removed periodically from each sample, acidified with 1% (v/v) trifluoroacetic acid (TFA), and then lyophilized. Peptide digestion was monitored by reverse phase HPLC. To do so, lyophilizates were first dissolved in concentrated formic acid, sonicated for 5 min at ambient temperature, diluted 10-fold with 0.1% TFA/2% acetonitrile in water, then chromatographed on a Vydac C4 column using a 55 min gradient of 0–58% acetonitrile in 0.1% TFA.

Circular dichroism spectroscopy. αtα solutions (60 μM) were prepared using either: 5 mM glycine-HCl, pH 3.6, 100 mM sodium fluoride (NaF); 5 mM sodium phosphate, pH 7.4, 100 mM NaF; or 5 mM glycine-NaOH, pH 10.5, 100 mM NaF. Spectra were recorded as described[30]. Temperature unfolding curves were obtained by monitoring ellipticity at 222 nm. Temperature intervals of 5 °C were used. At each temperature, the sample was equilibrated for 5 min prior to measurement. CD spectra in Fig. 4 were obtained after 0, 2, 3, 4 and 5 days of incubation at 37 °C using a 25 μM solution of αtα in 5 mM phosphate, pH 7.4, 100 mM NaF.

LDH assay. LDH release from mixed primary rat neuronal cultures was studied as described[30]. Briefly, Aβ(1–40) and αtα peptides were pre-incubated at a concentration of 500 μM in 20 mM HEPES, pH 7.4, for 0 or 3 days (Aβ), or for 0, 1, 3, or 6 days (αtα). The peptides were then diluted 10-fold in 50 μl of culture medium (final peptide concentration, 50 μM) before addition to the neuronal cells.

MTT assay. Reduction of MTT by PC12 cells was assayed as described[4]. Briefly, peptides were preincubated at a concentration of 250 μM in 20 mM HEPES, pH 7.4, at 37 °C for two days, then diluted in 50 μl of PC12 culture medium to yield final peptide concentrations of 0.001, 0.01, 0.1, 1, 10 and 20 μM, before addition to PC12 cells.

Acknowledgments

We thank C. Lemere for assistance with the birefringence experiment, A. Bissello for performing mass spectroscopy, S. Vasquez for preparation of primary neuronal cultures, and M. Condron for peptide synthesis and amino acid analysis. This work was supported by grants from the National Institutes of Health (D.B.T., D.J.S., and Y.F.), and by the Foundation for Neurologic Diseases (D.B.T and D.J.S.).

Correspondence should be addressed to Y.F. e*mail: fezoui@cnd.bwh.harvard.edu* or D.B.T. *email: teplow@cnd.bwh.harvard.edu*

Received 5 June, 2000; accepted 13 September, 2000.

1. Kelly, J.W. *Curr. Opin. Struct. Biol.* **8,** 101–106 (1998).
2. Pike, C.J., Burdick, D., Walencewicz, A.J., Glabe, C.G. & Cotman, C.W. *J. Neurosci.* **13,** 1676–1687 (1993).
3. Lambert, M.P. *et al. Proc. Natl. Acad. Sci. USA* **95,** 6448–6453 (1998).
4. Walsh, D.M. *et al. J. Biol. Chem.* **274,** 25945–25952 (1999).
5. Hartley, D.M. *et al. J. Neurosci.* **19,** 8876–8884 (1999).
6. Chiti, F. *et al. Proc. Natl. Acad. Sci. USA* **96,** 3590–3594 (1999).
7. Guijarro, J.I., Sunde, M., Jones, J.A., Campbell, I.D. & Dobson, C.M. *Proc. Natl. Acad. Sci. USA* **95,** 4224–4228 (1998).
8. Gross, M. *et al. Protein Sci.* **8,** 1350–1357 (1999).
9. Fezoui, Y., Weaver, D.L. & Osterhout, J.J. *Proc. Natl. Acad. Sci. USA* **91,** 3675–3679 (1994).
10. Fezoui, Y., Connolly, P.J. & Osterhout, J.J. *Protein Sci.* **6,** 1869–1877 (1997).
11. Goldsbury, C.S. *et al. J. Struct. Biol.* **119,** 17–27 (1997).
12. Harper, J.D. & Lansbury, P.T., Jr. *Annu. Rev. Biochem.* **66,** 385–407 (1997).
13. Glenner, G.G. *Prog. Histochem. Cytochem.* **13,** 1–37 (1981).
14. Fezoui, Y., Braswell, E.H., Xian, W. & Osterhout, J.J. *Biochemistry* **38,** 2796–2804 (1999).
15. Chakrabartty, A., Kortemme, T. & Baldwin, R.L. *Protein Sci.* **3,** 843–852 (1994).
16. Fezoui, Y., Weaver, D.L. & Osterhout, J.J. *Protein Sci.* **4,** 286–295 (1995).
17. Lumb, K.J. & Kim, P.S. *Science* **268,** 436–439 (1995).
18. Zhou, N.E., Kay, C.M. & Hodges, R.S. *Protein Eng.* **7,** 1365–1372 (1994).
19. Kuwajima, K. In *Circular dichroism and the conformational analysis of biomolecules* (ed., Fasman, G.D.) 159–182 (Plenum Press, New York; 1996).
20. Harrison, P.M., Bamborough, P., Daggett, V., Prusiner, S.B. & Cohen, F.E. *Curr. Opin. Struct. Biol.* **7,** 53–59 (1997).
21. Lai, Z., Colon, W. & Kelly, J.W. *Biochemistry* **35,** 6470–6482 (1996).
22. Booth, D.R. *et al. Nature* **385,** 787–793 (1997).
23. Takahashi, Y., Ueno, A. & Mihara, H. *Bioorg. Med. Chem.* **7,** 177–185 (1999).
24. Mihara, H., Takahashi, Y. & Ueno, A. *Biopolymers* **47,** 83–92 (1998).
25. Takahashi, Y., Ueno, A. & Mihara, H. *Chem. Eur. J.* **4,** 2475–2484 (1998).
26. Geula, C. *et al. Nature Med.* **4,** 827–831 (1998).
27. Abe, K. & Saito, H. *Brain Res.* **830,** 146–154 (1999).
28. Cooper, G.J. *et al. Proc. Natl. Acad. Sci. USA* **84,** 8628–8632 (1987).
29. Walsh, D.M., Lomakin, A., Benedek, G.B., Condron, M.M. & Teplow, D.B. *J. Biol. Chem.* **272,** 22364–22372 (1997).
30. Fezoui, Y. *et al. Amyloid: Int. J. Exp. Clin. Invest.* **7,** 166–178 (2000).
31. Koradi, R., Billeter, M. & Wuthrich, K. *J. Mol. Graphics* **14,** 51–55 (1996).